# SAR estimation in human head models related to TETRA, GSM and UMTS exposure using different computational approaches

IRENE KARANASIOU
Microwave and Fiber Optics Laboratory
School of Electrical and Computer Engineering
Institute of Communication and Computer Systems
National Technical University of Athens
9, Iroon Polytechniou,
157 73 Zografou Athens
ikaran@esd.ece.ntua.gr
GREECE
ikaran@esd.ece.ntua.gr

*Abstract:* - The scope of this paper is to calculate the electric field both inside and outside the human head and consequently to estimate the Specific Absorption Rate (SAR) when an antenna is placed at its close proximity at TETRA, UMTS and GSM frequencies. The analysis is twofold: a semi-analytical approach based on three-dimensional Green's function theory is initially implemented whereas a FEM (Finite Element Method) method is used in order to further validate the analysis, by simulating the relevant three-dimensional geometries. Numerical and simulation results are obtained for the local SAR values at different points inside the head when the model of the human head is exposed to the radiation of dipole antennas at 0.4GHz (TETRA), 0.9GHz (GSM), 1.8GHz (GSM) and 2.2GHz (UMTS) placed at a distance of 1 cm, 2cm and 3cm from the head model.

*Key-Words:* - mobile phones, GSM, UMTS, TETRA, Specific Absorption Rate, Green's function, Finite Element Method

## 1 Introduction

As the usage of mobile phones and other wireless devices increases in everyday life, so does the concern about potential health effects related to their use. Although national and international agencies have established safety guidelines for exposure to radiofrequency (RF) fields, concerns are still raised about the potential occurrence of adverse health effects in relation to RF field exposure. The International Commission on Non-Ionizing Radiation Protection (ICNIRP) and IEEE have provided guidelines specifying the safety limits for such exposure of RF radiation [1], [2]. In parallel the World Health Organization's agenda (WHO) is constantly updated to include all emerging new aspects concerning the biological implications of RF fields in public health [3]. Extensive studies reviewing recently reported results in literature also including inter-county research work are also being performed [4], [5].

The method generally used to assess the radiation of mobile phones is the measurement of the specific absorption rate (SAR). The SAR is an indication of the amount of electromagnetic energy absorbed by the biological tissues, and in the case in question, in the human body. Between 100 kHz and 6 GHz for RF fields, the Specific Absorption Rate (known as SAR) measured in Watts per kilogram (W/kg), is the fundamental RF dosimetry parameter and is defined as the rate of energy absorbed per unit mass. The SAR is determined by the incident electromagnetic waves and by the electrical and geometrical characteristics of the exposed object [6].

Researchers have used a number of different approaches to evaluate the interaction between the human head and mobile phone antennas. Some researchers implement numerical methods in conjunction with anatomically based models of the human body to study electromagnetic energy coupled to the head due to mobile telephones at different frequencies (e.g. [7], [8], [9]) and various antenna types (e.g. [10]), whereas others perform experimental studies of the SAR characteristics of

mobile phones (e.g. [11]]). In parallel a significant number of in vitro studies are also carried out (e.g. [12], [13])

Moreover, concerns have been raised associated with the temperature rise in head and brain tissues due to the use of cellular phones which has led to significant research work on this subject. Simple [14]-[16] or more complex thermal models [17]-[19] to compute the temperature rise as a result of calculated SAR distributions are used to this end. Also, numerous papers have been published focusing specifically on the comparison of specific absorption rates (SARs) in various anatomically detailed head models [20]-[23].

Mobile phone users in epidemiological studies have often used more than one phone model, and sometimes also more than one mobile phone system (analogue and digital systems). Additionally, experimental measurements of the SAR in live organisms are complicated and not always possible.

The present research focuses on using two theoretical approximations for the evaluation of the interaction between the human head and an antenna placed at its close proximity at four radiation frequencies at various antenna positions.

The two methodologies, used to calculate the electric field both inside and outside the head and consequently to estimate the Specific Absorption Rate (SAR) are: i. a semi-analytical approach based on two dimensional Green's function theory ii. a simulation tool using the FEM (Finite Element Method).

The analysis based on the Green's function theory, which is carried out using a customized simulation tool previously developed [24], [25], is valuable since it represents the worst case due to its more simplified modeling whereas the use of the FEM tool and the anatomical head model used provides more detailed and realistic results.

In the present analysis in order to model the human head a double-layered sphere is used in the Green's function analysis and an anatomical head model is used in the FEM analysis. The various layers are used to simulate the behavior of different biological media; bone and brain (gray matter) tissues. Numerical and simulation results are obtained for the local SAR values at different points inside the head when the model of the human head is exposed to the radiation of antennas at 0.4 GHz (TETRA), 0.9 GHz (GSM), 1.8 GHz (GSM) and 2.2 GHz (UMTS) placed at a distance of 1 cm, 2cm and 3cm from the head model.

## 2 Materials and Methods

The geometry of the problem is depicted in Fig. 1. The head is modeled by a double-layered sphere with radii a1 and a2. The two layers are used to simulate different biological media; bone and brain (gray matter) tissues. The regions (1) and (2) have dielectric constants ε1 and ε2 respectively. The region (3) represents the free space with dielectric constant ε0. The system is excited by an antenna placed outside the head model where the antenna's axis is considered parallel to z-axis.

Green's function in each region i=1, 2, 3 of space is properly expanded to an infinite sum of spherical waves satisfying the appropriate vector wave equation. By virtue of the spherical symmetry of the problem, spherical coordinates are used, with unit vectors $\hat{r},\ \hat{n},\ \hat{\varphi}$.

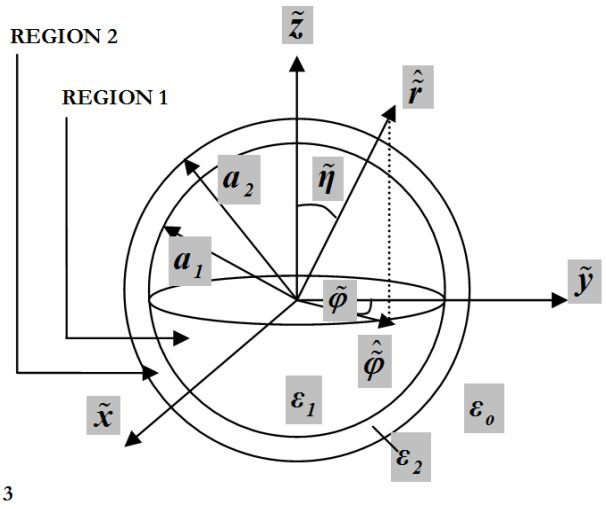


Figure 1. The geometry of the problem

The following expressions describe the electric-type Green's function in the three regions of space.

Region 1

$$\underline{\underline{\dot{G}}}_1(\tilde{\underline{r}},\tilde{\underline{r}}') = \sum_{n=1}^{\infty}\sum_{m=-n}^{n}\left[\underline{m}_{mn}^{(1)}(\tilde{\underline{r}},k_1)\underline{a}_{mn}(\tilde{\underline{r}}') + \underline{n}_{mn}^{(1)}(\tilde{\underline{r}},k_1)\underline{a}'_{mn}(\tilde{\underline{r}}')\right], \quad \tilde{r} \le a_1 \qquad (1)$$

Region 2

$$\overline{\underline{G}}_2(\underline{\tilde{r}},\underline{\tilde{r}}') = \sum_{n=1}^{\infty}\sum_{m=-n}^{n}\Big[(\underline{m}_{mn}^{(1)}(\underline{\tilde{r}},k_2)\underline{b}_{mn}(\underline{\tilde{r}}')+\underline{n}_{mn}^{(1)}(\underline{\tilde{r}},k_2)\underline{b}'_{mn}(\underline{\tilde{r}}'))+(\underline{m}_{mn}^{(2)}(\underline{\tilde{r}},k_2)\underline{c}_{mn}(\underline{\tilde{r}}')+\underline{n}_{mn}^{(2)}(\underline{\tilde{r}},k_2)\underline{c}'_{mn}(\underline{\tilde{r}}'))\Big], \quad \tilde{r}\le a_2 \qquad (2)$$

where $k_i = k_o\sqrt{\varepsilon_i}$, $\underline{a}_{mn}(\underline{\tilde{r}}')$, $\underline{a}'_{mn}(\underline{\tilde{r}}')$,…, $\underline{c}'_{mn}(\underline{\tilde{r}}')$ are unknown coefficients to be determined and $\underline{m}_{mn}^{(j)}(\underline{\tilde{r}},k_i)$, $\underline{n}_{mn}^{(j)}(\underline{\tilde{r}},k_i)$, *i =1, 2; j = 1, 2* are the well known spherical wave functions.

Regarding, the region outside the head and inside the ellipsoidal cavity, the electric field consists of the primary excitation $\overline{\underline{G}}_0(\underline{\tilde{r}},\underline{\tilde{r}}')$ from the unit source located at $\underline{\tilde{r}}'$ and the contribution of the field $\overline{\underline{G}}_s(\underline{\tilde{r}},\underline{\tilde{r}}')$, scattered from the double layered sphere. Thus,

Region 3

$$\overline{\underline{G}}_3(\underline{\tilde{r}},\underline{\tilde{r}}') = \overline{\underline{G}}_0(\underline{\tilde{r}},\underline{\tilde{r}}') + \overline{\underline{G}}_s(\underline{\tilde{r}},\underline{\tilde{r}}') \qquad (3)$$

where, $\overline{\underline{G}}_0(\underline{\tilde{r}},\underline{\tilde{r}}')$ is the free space dyadic Green's function and is defined by an infinite sum of spherical waves as

$$\overline{\underline{G}}_0(\underline{\tilde{r}},\underline{\tilde{r}}') = \sum_{n=1}^{\infty}\sum_{m=-n}^{n}(-1)^m\frac{-jk_0}{4\pi}\frac{2n+1}{n(n+1)}\cdot \times\begin{cases}\underline{m}_{-mn}^{(1)}(\underline{\tilde{r}},k_0)\underline{m}_{mn}^{(3)}(\underline{\tilde{r}}',k_0)+\underline{n}_{-mn}^{(1)}(\underline{\tilde{r}},k_0)\underline{n}_{mn}^{(3)}(\underline{\tilde{r}}',k_0), & \tilde{r}>\tilde{r}'\\ \underline{m}_{-mn}^{(3)}(\underline{\tilde{r}},k_0)\underline{m}_{mn}^{(1)}(\underline{\tilde{r}}',k_0)+\underline{n}_{-mn}^{(3)}(\underline{\tilde{r}},k_0)\underline{n}_{mn}^{(1)}(\underline{\tilde{r}}',k_0), & \tilde{r}<\tilde{r}'\end{cases} \qquad (4)$$

Hereupon, the unknown expansion coefficients of the infinite sum of spherical waves are determined by the boundary conditions on the interfaces $\tilde{r}=a_1,\ a_2$. In order to satisfy the continuity of the tangential electric and magnetic field components, the boundary conditions on the interfaces $\tilde{r}=a_1,\ a_2$ are then imposed by implementing the expressions:

$$\hat{\tilde{r}}\times\overline{\underline{G}}_i(\underline{\tilde{r}},\underline{\tilde{r}}') = \hat{\tilde{r}}\times\overline{\underline{G}}_{i+1}(\underline{\tilde{r}},\underline{\tilde{r}}'), \quad \tilde{r}=a_i;\ i=1,\ 2 \qquad (5)$$

$$\hat{\tilde{r}}\times(\nabla\times\overline{\underline{G}}_i(\underline{\tilde{r}},\underline{\tilde{r}}')) = \hat{\tilde{r}}\times(\nabla\times\overline{\underline{G}}_{i+1}(\underline{\tilde{r}},\underline{\tilde{r}}')), \quad \tilde{r}=a_i;\ i=1,\ 2 \qquad (6)$$

where $\hat{\tilde{r}}$ denotes the unit vector along the radial direction of the local coordinate system (Fig.1). By implementing the orthogonality properties of the spherical wave functions, two independent 4 x 4 linear sets of equations are obtained for the unknown expansion coefficients stated above. These two independent sets can be solved analytically for the coefficients $\underline{a}_{mn}(\underline{\tilde{r}}')$, $\underline{b}_{mn}(\underline{\tilde{r}}')$, $\underline{c}_{mn}(\underline{\tilde{r}}')$ and $\underline{a}'_{mn}(\underline{\tilde{r}}')$, $\underline{b}'_{mn}(\underline{\tilde{r}}')$, $\underline{c}'_{mn}(\underline{\tilde{r}}')$ respectively.

The electric field at a point $\vec{r}$ lying in any region is given by:

$$\vec{E}_i(\vec{r}) = \omega\ \mu_0 I_0 G_i(\vec{r}) \qquad (7)$$

where i=1,2,3, $G_i(\vec{r})$ is the Green's function in the corresponding region and $I_0$ is given by the following equation:

$$I_0 = \frac{1}{\omega\mu_0}\sqrt{\frac{(1Watt)16z_0k_0}{\lambda}} \qquad (8)$$

where $z_0 = \sqrt{\frac{\mu_0}{\varepsilon_0}}$ and $k_0 = \frac{2\pi}{\lambda}$.

The SAR at a point $\vec{r}$ inside the head is given by the following equation:

$$SAR(\vec{r}) = \frac{\sigma(\vec{r})\,|\underline{E}(\vec{r})|^2}{\rho(\vec{r})} \quad \text{(Watt/kgr)} \qquad (9)$$

where σ (S/m) is the conductivity, ρ (kgr/m$^3$) is the density of the tissue and $|E(\vec{r})|$ is the magnitude of the electric field (V/m) [26].

The investigation of the electromagnetic problem is approached also numerically using commercial simulation software (*HFSS*, *H*igh *F*requency *S*tructure *S*imulator, Ansoft Corporation). HFSS solves Maxwell's equations using a finite element method, in which the solution domain is divided into a set of tetrahedral elements, termed as "mesh." The characteristics of the generated mesh, which are fully automatically optimized, are crucial to

obtaining a reliable, well-converged solution. In order to obtain a converged solution a criterion was established: the error of the systems S parameters between two successive passes should be less than 0.02. In all the results presented the above criterion was achieved. The head model used is an anatomical meshed head model.

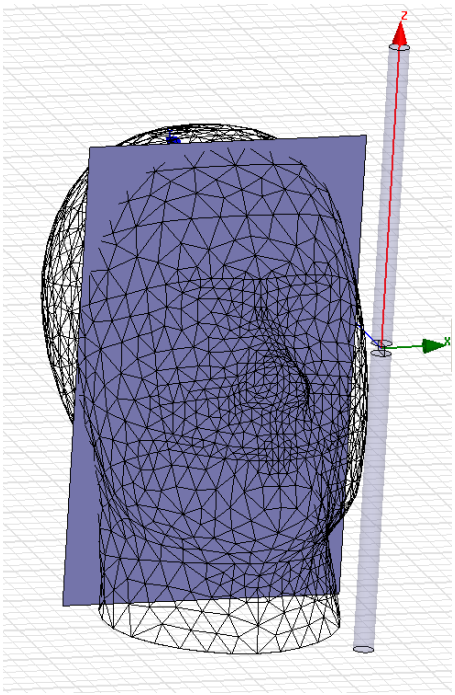

Figure 2. Anatomical head model used in FEM simulator

## 3 Numerical Results

Numerical results are presented after calculation using the frequencies $f_1$=0.4GHz (TETRA), $f_2$=0.9GHz (GSM), $f_3$=1.8GHz (GSM) and $f_4$=2.2GHz (UMTS). The head model, including skull and brain (gray matter) is of total diameter 10cm and hence the radii of the two cylinders are $\alpha_1$=4cm and $\alpha_2$=1cm.The dielectric properties of the tissue composition used for the computation are reported in literature for each frequency [27]. The magnetic properties of the layers are denoted as $\mu_1=\mu_2=\mu_0=4\pi 10^{-7}$ Henry/m. The antenna was placed at a distance of 1, 2, 3cm from the ear oriented in parallel to the z-axis.

The penetration curves, which are the SAR values variation from “one ear to the other” along the longitudinal x-axis have been computed at each antenna operating frequency, when the antenna is placed at the above mentioned distances, and the results are shown in the following figure (Fig. 3).

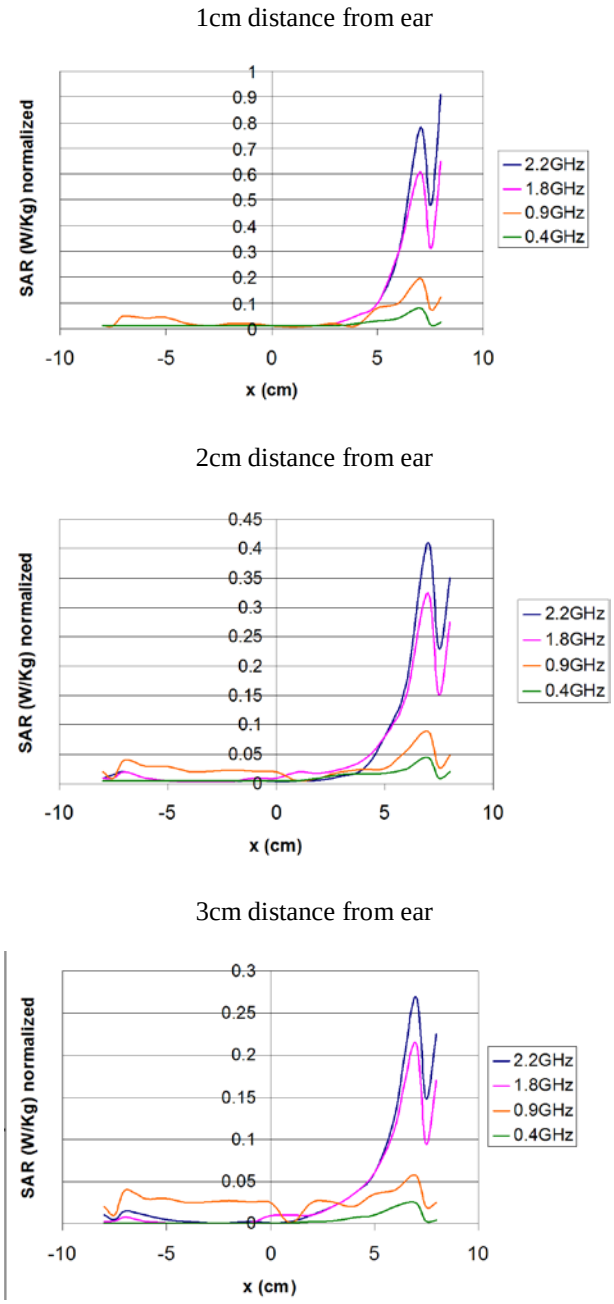


Figure 3. Variation of SAR along x-axis of spherical head model

As expected from theory the SAR values are larger as frequency increases while penetration depth decreases with increasing frequency. The SAR distributions seem to be smoother at lower frequencies whereas abrupt peaks of SAR values are observed at the higher frequencies. Also, large SAR values are observed on the head-air interface at high frequencies (1.8 GHz and 2.2GHz) due to the immediate change of the refraction index from the value 1 in air to a much larger value in brain gray matter.

Following, the local SAR using the FEM tool has been computed inside the head model at each

frequency, at each of the aforementioned distances and the results are shown in the following figures 4 to 9. The maximum SAR values observed are also calculated.

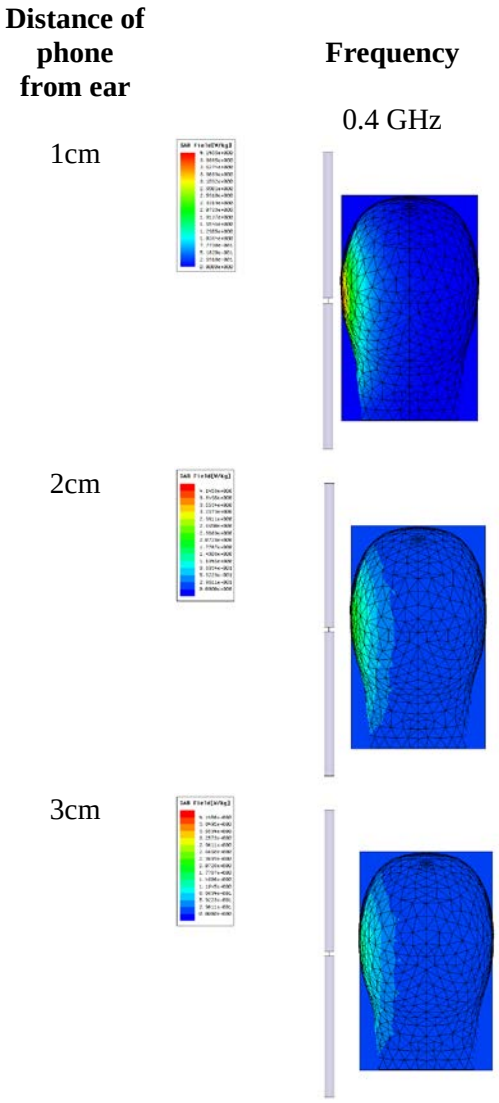


Max value: 4.15 W/Kg

Figure 4. Normalized SAR distribution at 0.4GHz

By observation of the results deriving by implementation of both methodologies, the maximum local SAR value is dependent on the frequency and type of signal. The maximum local SAR values at 2.2GHz are larger than those at 1.8GHz, the maximum local SAR values at 1.8GHz are larger than those at 0.9GHz and finally the maximum local SAR values at 0.9GHz are larger than those at 0.4GHz for the same radiated power of 1Watt. Once again it is observed that the penetration depth decreases as the frequency increases.

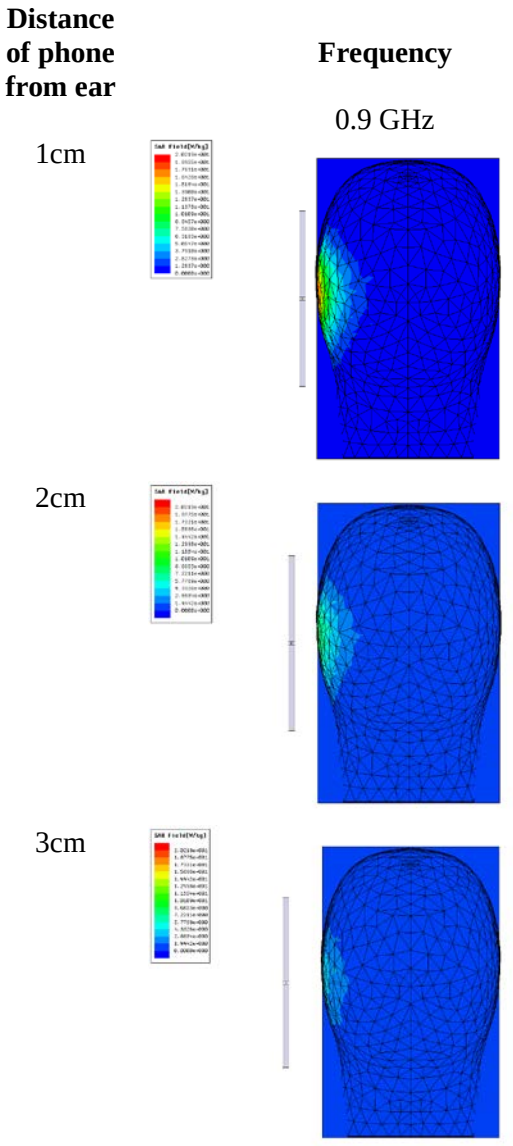


Max value: 20.22 W/Kg

Figure 5. Normalized SAR distribution at 0.9GHz

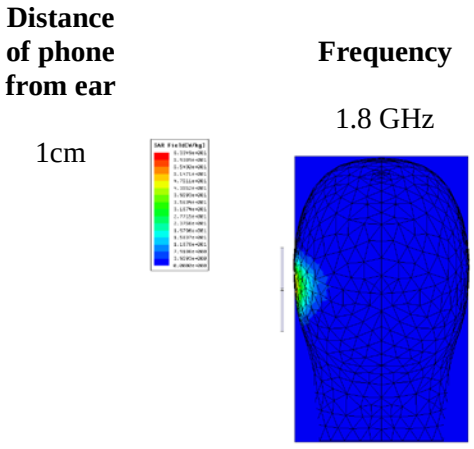

2cm

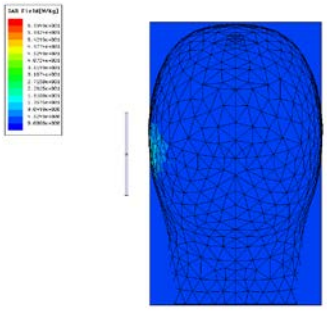

3cm

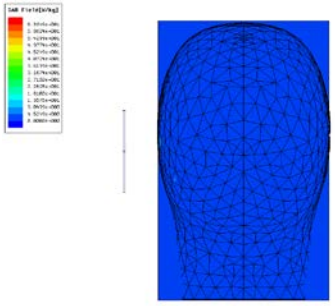

Max value: 63.35 W/Kg

Figure 6. Normalized SAR distribution at 1.8 GHz

As also expected, the maximum local SAR value is dependent on the distance between the antenna and the head. The maximum local SAR values when the antenna's distance from the head is 1cm are larger than those when this distance is 2 cm and the latter are larger than those when the distance in question is 3 cm at the same operation frequency and for the same antenna radiated power of 1W.

| **Distance of phone from ear** | **Frequency** 2.2 GHz |
|---|---|
| 1cm | 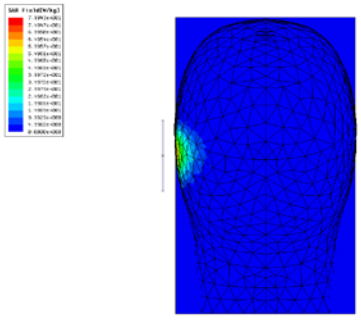 |
| 2cm | 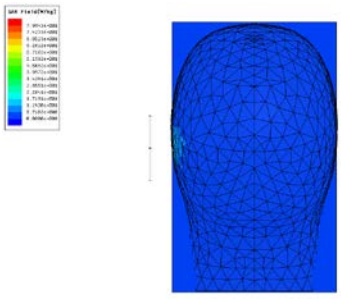 |
| 3cm | 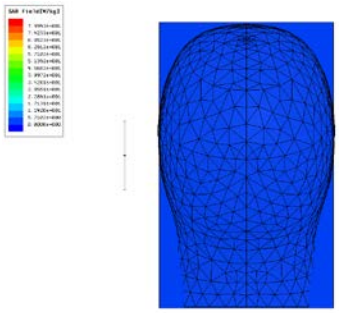 |

Max value: 79.94 W/Kg

Figure 7. Normalized SAR distribution at 2.2 GHz

By observing figs. 6 and 7, it is concluded that the results for the higher frequencies are similar. The SAR distributions present maximum values close the human ear, near the surface of the human head model and the maximum SAR values are also similar. As the antenna is placed away from the head model the SAR is minimized.

At lower frequencies, larger areas of the human head model are radiated and the penetration depth is larger than that observed at the two highest frequencies.

| Normalized SAR value at the lowest frequency | linear | logarithmic |
|---|---|---|
| 0.4GHz | 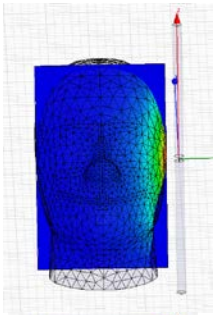 | 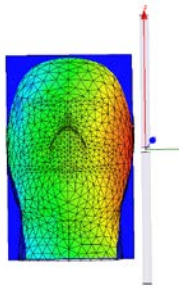 |
| 0.9GHz | 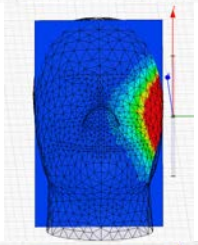 | 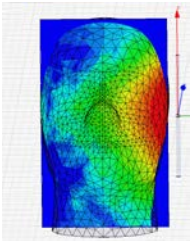 |
| 1.8GHz | 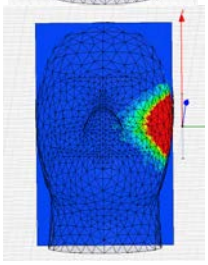 | 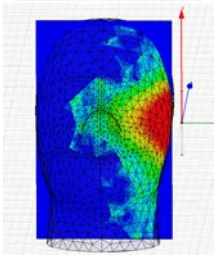 |

2.2GHz

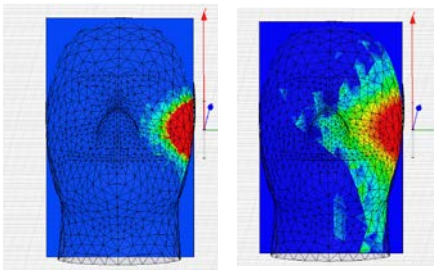

Figure 8. Normalized SAR distribution (at the lowest frequency) at both linear and logarithmic scales.

In order to easily compare the results by observation and also exhibit the differences between frequencies, the SAR distributions have been normalized based on min and max observed values at 1cm distance of antenna from ear both at linear and logarithmic scales.

All figures present the SAR distributions at a xy plane at a transversal cut at the ear of the head model, which is the area where the mobile phone is in general held and where its antenna radiates.

Normalized SAR value at highest frequency

logarithmic

0.4GHz

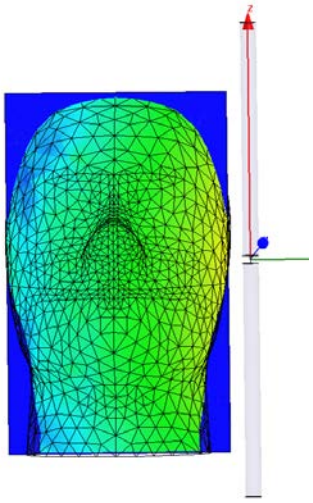

0.9GHz

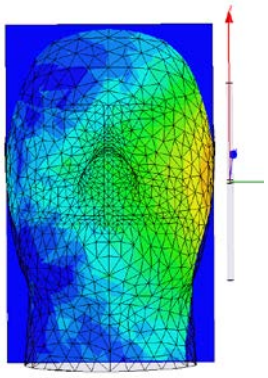

1.8GHz

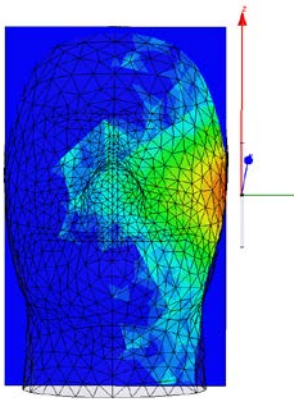

2.2GHz

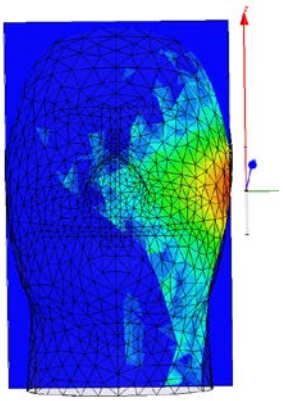

Figure 9. Normalized SAR distribution (at the highest frequency) at logarithmic scale

Once again similar results regarding head model radiated areas, penetration depths and maximum SAR values versus frequency range are obtained.

## 4 Discussion and Conclusion

In the present study the interaction between the human head model and a mobile antenna at four operating frequencies has been studied using a semi-analytical Green's function technique and the FEM method, mainly in order to validate the performance of the fast semi-analytical method.

Based on the simulation results in all cases, in terms of use of a mobile phone, it could be assumed that the higher the frequency used and the smaller the distance is from the human head, the higher the exposure. Nevertheless, at high frequencies the penetration depth observed is small.

Although there are large differences mainly in geometry, shape and tissue distribution in the examined configurations, the SAR distributions are quite similar. Quantitative differences in SAR values are mainly caused by differences in the head anatomy and the distance of the closest tissue tetrahedral to the antenna as well as the methodology used for the analysis. The results of this study confirm the earlier results indicating that

SAR values are sensitive to parameters, such as distance of current source, anatomical structure of the head model and frequency [28]-[30].

It should always be kept in mind that several RF fields appear to be associated with certain biological effects of unknown clinical significance that require clarification. Up to now there isn't any clear evidence of adverse health effects associated with RF fields from mobile phones. Given also the outburst of new technologies, extensive and continuous research is needed to address long-term exposure and to gradually follow various possible health effects right from the very early stages of their appearance. RF exposure guidelines are also updated as new scientific information on RF fields and health risks is generated.

It is worth mentioning that not many studies exist for the TETRA operating frequency regarding its potential biological effects in humans. Exposure to a continuous wave signal around 400MHz having TETRA signal characteristics, doesn't seem to affect users nor seems to be responsible for symptoms reported by some TETRA users [31]. Nevertheless, exposure to a continuous wave signal may affect symptoms and should be further investigated [32].

Another parameter that could be studied as a factor of potential biological importance in risk assessment radiofrequency (RF) communication systems and other technologies is modulation. Modulation introduces a spread of frequencies into the carrier signal, but in general when compared to the frequency of the carrier, this spread is rather small. While a variety of modulation-dependent biological effects of RF energy have been reported, the underlying biological mechanisms have not been determined [33].

Nevertheless, evidence that pulse-modulated RF EMF alters brain physiology as measured in EEG studies has been reported but without clear exposure-related effects in cognitive performance [33].

Finally, it has been long investigated over the last five decades whether non-thermal biological effects of RF frequencies exist. Numerous in vitro and in vivo studies have been reported over the years [34]. It has been concluded so far that the key pathways towards the understanding of such mechanisms rely on using multiscale approaches based on affordable and realistic in silico models [34].

ACKNOWLEDGEMENT
The author would like to thank Mrs. Maria Koutsoupidou for her valuable comments regarding the modeling of the problem.

*References:*

[1] ICNIRP, "Guidelines for limiting exposure to time-varying electric, magnetic, and electromagnetic fields (up to 300 GHz)", *Health Phys* Vol. 74, pp. 494–552, 1998.

[2] IEEE C95.1-1999, "Safety levels with respect to human exposure to radio frequency electromagnetic fields: 3 kHz to 300 GHz", *IEEE standard*, 1999.

[3] Deventer, van E. et al.. WHO Research Agenda for Radiofrequency Fields. *Bioelectromagnetics* vol. 32, pp. 417-421, 2011.

[4] Foster, K.R., Moulder, J.E. Wi-Fi and health: Review of current status of research *Health Physics*, vol. 105, No. 6, pp. 561-575, 2013

[5] Cardis, E., Armstrong, B.K., Bowman, J.D., Giles, G.G., Hours, M., Krewski, D., McBride, M., Parent, M.E., Sadetzki, S., Woodward, A., Brown, J., Chetrit, A., Figuerola, J., Hoffmann, C., Jarus-Hakak, A., Montestruq, L., Nadon, L., Richardson, L., Villegas, R., Vrijheid, M. Risk of brain tumours in relation to estimated RF dose from mobile phones: Results from five interphone countries *Occupational and Environmental Medicine*, Vol. 68, No. 9, pp. 631-640, 2011.

[6] Gandhi, O.P. Lazzi, G. Furse, C.M., "Electromagnetic absorption in the human head and neck for mobile telephones at 835 and 1900 MHz" , *IEEE Transactions on Microwave Theory and Techniques*, Vol. 44, No. 10, Part 2 pp.1884-1897, Oct 1996.

[7] Manteuffel, D. Bahr, A. Waldow, P. Wolff, I. IMST GmbH, Kamp-Lintfort; "Numerical analysis of absorption mechanisms for mobile phones with integrated multiband antennas" *IEEE Antennas and Propagation Society* International Symposium, Vol.3, pp. 82-85, 2001.

[8] Piuzzi, E. et al.. Analysis of Adult and Child Exposure to Uniform Plane Waves at Mobile Communication Systems Frequencies (900 MHz–3 GHz). *IEEE Trans. Electr. Compat.*, Vol. 53, No.1, pp. 38 – 47, 2011.

[9] Andreas Christ et al. The Virtual Family—development of surface-based anatomical models of two adults and two children for dosimetric simulations *Phys. Med. Biol.* 55 N23, 2010.

[10] Chan, K. H., Leung, S. W., Fung, L. C. and Siu, Y. M. "Experimental study of the sar characteristics of mobile phones," *Microwave and Optical Technology Letters*, Vol. 40, No. 1, Jan. 2004

[11] Kuehn, S., Kelsh, M. A., Kuster, N., Sheppard, A. R. and Shum, M., Analysis of mobile phone design features affecting radiofrequency power absorbed in a human head phantom. *Bioelectromagnetics*, Vol. 34, pp. 479–488, 2013.

[12] Rammal, M., Jebai, F., Rammal, H., Joumaa, W.H. Effects of long-term exposure to RF/MW radiations on the expression of mRNA of stress proteins in Lycospersicon esculentum. *WSEAS Transactions on Biology and Biomedicine*, 11, pp. 10-14, 2014.

[13] Paffi, A., Apollonio, F., Lovisolo, G.A., Marino, C., Pinto, R., Repacholi, M., Liberti, M. Considerations for developing an RF exposure system: A review for in vitro biological experiments *IEEE Transactions on Microwave Theory and Techniques*, Vol. 58 No. 10, art. no. 5570973, pp. 2702-2714, 2010.

[14] Wang J and Fujiwara O "FDTD computation of temperature rise in the human head for portable telephones" *IEEE Trans. Microw. Theory Tech.* Vol. 47, pp. 1528–34, 1999.

[15] Wainwright P R "Thermal effects of radiation from cellular phones" *Phys. Med. Biol*. Vol. 45 pp. 2363–72, 2000.

[16] Gandhi O P, Li Q X and Kang G "Temperature rise for the human head for cellular telephones and for peak SARs prescribed in safety guidelines" *IEEE Trans. Microw. Theory Tech*. Vol. 49, pp. 1607–13, 2001.

[17] Van Leeuwen G M J, Lagendijk J J W, Van Leersum B J A M, Zwamborn A P M, Hornsleth S N and Kotte A N T J "Calculation of change in brain temperatures due to exposure to a mobile phone" *Phys. Med. Biol.* Vol. 44, pp. 2367–79,1999.

[18] J B Van de Kamer and J JW Lagendijk, "Computation of high-resolution SAR distributions in a head due to a radiating dipole antenna representing a hand-held mobile phone", *Phys. Med. Biol*. Vol. 47, pp. 1827–1835, 2002.

[19] Murbach, M., Neufeld, E., Christopoulou, M., Achermann, P. and Kuster, N. Modeling of EEG electrode artifacts and thermal ripples in human radiofrequency exposure studies. *Bioelectromagnetics*, Vol. 35, pp. 273–283, 2014.

[20] Ae-Kyoung Lee, Hyung-Do Choi, and Jae-Ick Choi, "Study on SARs in Head Models with Different Shapes by Age Using SAM Model for Mobile Phone Exposure at 835 MHz", *IEEE Transactions on electromagnetic compatibility*, Vol. 49, No. 2, 302-312, May 2007

[21] J.Wang and O. Fujiwara, "Comparison and evaluation of electromagnetic absorption characteristics in realistic human head models of adult and children for 900 MHz mobile telephones," *IEEE Trans. Microw. Theory Tech*., Vol. MTT-51, No. 3, pp. 966–971, Mar. 2003.

[22] A. Hadjem, D. Lautru, C. Dale, M. F. Wong, V. F. Hanna, and J. Wiart, "Study of specific absorption rate (SAR) induced in two child head models and in adult heads using mobile phones," *IEEE Trans. Microw. Theory Tech*., Vol. 53, No. 1, pp. 4–11, Jan. 2005.

[23] G. Bit-Babik, A. W. Guy, and C.-K Chou et al., "Simulation of exposure and SAR estimation for adult and child heads exposed to radiofrequency energy from portable communication devices," *Radiat. Res.*, Vol. 163, pp. 580–590, May 2005.

[24] Irene S. Karanasiou, Nikolaos K. Uzunoglu and Anastasios Garetsos, "Electromagnetic Analysis of a Non-invasive 3D Passive Microwave Imaging System" *Progress in Electromagnetic Research*, PIER 44, pp. 287-308, 2004.

[25] Irene S. Karanasiou, Nikolaos K. Uzunoglu and Charalabos Papageorgiou, "Towards functional non-invasive imaging of excitable tissues inside the human body using Focused Microwave Radiometry", Special Issue on "Biological Effects and Medical Applications of RF/Microwaves" of the *IEEE Transactions on Microwave Theory and Techniques*, Vol. 52, No. 8, pp. 1898-1908, Aug. 2004.

[26] Nikita, K.S.; Stamatakos, G.S.; Uzunoglu, N.K.; Karafotias, A., "Analysis of the interaction between a layered spherical human head model and a finite-length dipole," *Microwave Theory and Techniques, IEEE Transactions on*, Vol.48, No.11, pp.2003, 2013, Nov 2000.

[27] C. Gabriel, "Compilation of the Dielectric Properties of Body Tissues at RF and Microwave Frequencies", Brooks Air Force Technical Report AL/OE-TR-1996-0037.

[28] J Keshvari and S Lang, "Comparison of radio frequency energy absorption in ear and eye region of children and adults at 900, 1800 and

2450 MHz", *Phys. Med. Biol.* Vol. 50, pp. 4355–4369, 2005.

[29] Burkhardt M and Kuster N "Review of exposure assessment for handheld mobile communications devices and antenna studies for optimized performance", Review of Radio Science 1996–1999 ed W R Stone (Oxford, UK: Oxford University Press) chapter 34, 1999.

[30] Okoniewski, M.; Stuchly, M.A. "A study of the handset antenna and human body interaction" *Microwave Theory and Techniques, IEEE Transactions on* Vol. 44, No 10, pp. 1855 – 1864, Oct 1996.

[31] Rosa Nieto-Hernandez, J. Williams, A. J Cleare, S. Landau, S. Wessely, G James Rubin, Can exposure to a terrestrial trunked radio (TETRA)-like signal cause symptoms? A randomised double-blind provocation study *Occup Environ Med* Vol. 68, pp.339-344, 2011.

[32] Kenneth R. Foster and Michael H. Repacholi (*2004*) Biological Effects of Radiofrequency Fields: Does Modulation Matter?. *Radiation Research*: August 2004, Vol. 162, No. 2, pp. 219-225.

[33] Marc R. Schmid, Sarah P. Loughran1,Sabine J. Regel, Manuel Murbach, Aleksandra Bratic Grunauer, Thomas Rusterholz1, Alessia Bersagliere, Niels Kuster, Peter Achermann, Sleep EEG alterations: effects of different pulse-modulated radio frequency electromagnetic fields, *Journal of Sleep Research*, Vol. 21, No 1, pp. 50–58, February 2012.

[34] Apollonio, F. Liberti, M., Paffi, A., Merla, C. , Marracino, P., Denzi, A., Marino, C., d'Inzeo, G. Feasibility for Microwaves Energy to Affect Biological Systems Via Nonthermal Mechanisms: A Systematic Approach *Microwave Theory and Techniques, IEEE Transactions on* , Vol. 61 , No. 5, pp. 2031 – 2045, May 2013.